Inorganic Chemistry

Article

pubs.acs.org/IC

Red-Emitting $[Ru(bpy)_2(N\text{-}N)]^{2+}$ Photosensitizers: Emission from a Ruthenium(II) to 2,2′-Bipyridine ^{3}MLCT State in the Presence of Neutral Ancillary "Super Donor" Ligands

Amlan K. Pal,[†] Samik Nag,[‡] Janaina G. Ferreira,[†] Victor Brochery,[†] Giuseppina La Ganga,[§] Antonio Santoro,[§] Scolastica Serroni,[§] Sebastiano Campagna,*[,§] and Garry S. Hanan*[,†]

[†]Département of Chemistry, Université de Montréal, Montréal, Québec H3T-1J4, Canada

[‡]Department of Chemical Sciences, Sikkim University, Sixth Mile, Tadong, Gangtok, Sikkim, India 737102

[§]Dipartimento di Scienze Chimiche, Università di Messina, Via Sperone 31, I-98166 Messina, Italy

Supporting Information

ABSTRACT: The synthesis and characterization of a novel family of $[Ru^{II}(bpy)_2(N\text{-}N)](PF_6)_2$ (bpy = 2,2′-bipyridine) complexes are reported, where N-N = pyridine/pyrimidine/pyrazine functionalized in different positions with the electron-donating bicyclic hexahydropyrimidopyrimidine (hpp) unit. A series of bidentate ligands **1a**−**5a** were synthesized in good to high yields (55−96%). The corresponding complexes **1b**, **2b**, and **5b** were prepared in *n*-butanol, while complexes **3b** and **4b** were prepared in a mixture of *n*-butanol and water (1/1, v/v) in modest to good yields (23−76%). Both ligand and complex structures were fully characterized by a variety of techniques, including X-ray crystallography. In cyclic voltammetric studies, all the complexes exhibit a $Ru^{III/II}$ couple, which is ∼500 mV less positive than the $Ru^{III/II}$ couple in $Ru(bpy)_3^{2+}$. The ^{1}MLCT and ^{3}MLCT states of all of the complexes (530−560 nm/732−745 nm) are shifted bathochromically in comparison to those of $Ru(bpy)_3^{2+}$ (450 nm/620 nm). These values are in good agreement with DFT and TD-DFT calculations.

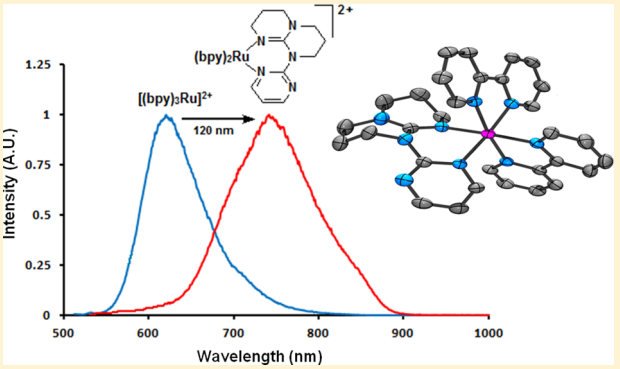

INTRODUCTION

For decades $Ru^{II}(bpy)_3$ (bpy = 2,2′-bipyridine) type complexes have attracted considerable interest because of their tunable photophysical properties[1a−e] as well as their potential for applications in water oxidation,[2] artificial photosynthesis,[3] and more generally in solar energy conversion.[3a,4] More recently, Ru(II)-based red-emitting photosensitizers with relatively long excited-state lifetimes have drawn attention, as they exhibit potential applications in biological systems[5] and as low-lying energy traps in multichromophore arrays.[6] The judicious choice of the ligands bonded to Ru(II) can tune the energy of the excited state,[7a−c] the excited-state lifetime,[1c,7,8] and the absorption energy of the complex,[7−9] while overcoming the limitation imposed by the energy gap law[7b,c] on the excited-state lifetime at the same time. Several strategies have been adopted by various groups to red-shift the absorption and emission of Ru(II)-heteroleptic complexes and to prolong their excited-state lifetimes; for example, (a) introduction of coplanar electron-withdrawing aromatic moiety containing bidiazine ligands bearing two-ring N heteroatoms,[10−14] thereby stabilizing the ^{3}MLCT state, (b) functionalization of bpy with various substituents in order to lower the LUMO,[15,16] (c) introduction of an organic chromophore to establish an equilibrium between the ^{3}MLCT and the organic chromophore triplet ^{3}LC states, (d) introduction of fused polyaromatic systems (benzoeilatin, 952 nm;[17] isoeilatin, 994 nm;[18] dipyridophenazine, 790 nm[19]), and (e) the formation of oligonuclear complexes with additional electron-withdrawing metal ions.[1,20] In general, the two principal approaches toward red-emitting Ru(II) complexes are (i) the incorporation of a better acceptor ligand,[15,16] in place of one bpy in $Ru(bpy)_3^{2+}$, thereby decreasing the energy of the LUMO of the new $Ru(bpy)_2(acceptor)^{2+}$ species, and (ii) introduction of a better donor ligand that functions by raising the energy of the HOMO in the new $Ru(bpy)_2(donor)^{2+}$ species.[21]

In a recent communication[21] we demonstrated that the presence of a strongly donating hpp unit attached to pyridine or pyrimidine units helps to red-shift the lowest energy ^{3}MLCT maxima of complexes **1b** and **3b** by about 100 nm in comparison to that of $Ru(bpy)_3^{2+}$. Herein, we report the complete synthesis and characterization of new, neutral bidentate ligands (**1a**−**5a**; Chart 1) and their $Ru(bpy)_2(L\text{-}L)^{2+}$ type (where L-L = ligands **1a**−**5a**) compounds **1b**−**5b**. The observed redox and photophysical properties are in good agreement with the density functional theory (DFT) and time-

Received: November 12, 2013
Published: January 13, 2014

   dx.doi.org/10.1021/ic4028332 | Inorg. Chem. 2014, 53, 1679−1689

Chart 1. 1,3,4,6,7,8-Hexahydro-2*H*-pyrimido[1,2-*a*]pyrimidine (H-hpp) Attached to Various N-Heterocycles: 2-Pyridyl (1a), 5-Bromo-2-pyridyl (2a), 2-Pyrimidyl (3a), 6-Chloro-4-pyrimidyl (4a), and 2-Pyrazyl (5a)

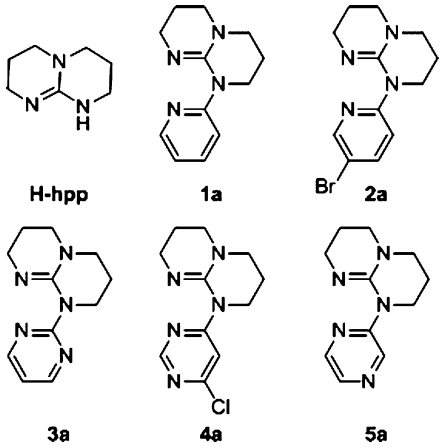

dependent density functional theory (TD-DFT) studies of the compounds.

RESULTS AND DISCUSSION

A series of substituted neutral bidentate N-heterocyclic ligands **1a-5a** (Chart 1) were synthesized by the reaction of 1,3,4,6,7,8-hexahydro-2*H*-pyrimido[1,2-*a*]pyrimidine (H-hpp) with various heterocycles (halo-pyridine/pyrimidine/pyrazine) by C−N bond forming reactions. Ligand **1a** was synthesized by a Pd-catalyzed Buchwald C−N cross-coupling reaction,[22] whereas the other ligands were synthesized by a neat reaction of the reactants at 90−130 °C or with the assistance of microwave heating at 160 °C. The ligands were also synthesized in neat reaction procedures, which provide a green route of using H-hpp as its own base and recuperating the relatively costly starting material by simple acid−base workup. Attaching a heterocycle to the guanidine N*H* position of H-hpp renders the six annular methylene units nonequivalent by both ^{1}H and ^{13}C NMR spectroscopy in contrast to free H-hpp, in which the tautomerization of the guanidine proton leads to only three proton resonances in its ^{1}H NMR at 400 MHz. Similar observations were reported by Coles and co-workers for a methylene-linked bis(guanidine) compound, $H_2C\{hpp\}_2$.[23]

Ligands **1a−5a** were characterized by high-resolution mass spectrometry, where the most abundant peaks were found to be $[M + H]^+$, with the $[M + 2H]^{2+}$ species (see the Experimental Section for details).

The stoichiometric reaction of **1a−5a** with *cis*-$Ru(bpy)_2Cl_2 \cdot 2H_2O$ in refluxing 1-butanol or a 1/1 (v/v) 1-butanol/H_2O mixture followed by the addition of aqueous NH_4PF_6 affords $[Ru(bpy)_2(\mathbf{1a-5a})](PF_6)_2$ (**1b−5b**) as dark red powders (Scheme 1). While compound **1b** could be isolated as a pure product without further purification, compounds **2b−5b** needed additional purification by column chromatography.

Complexes **1b−5b** were characterized by high-resolution mass spectrometry, where the most abundant peaks were found to be $[M]^{2+}$ in all cases. The $[M - PF_6]^+$ species could also be identified (see the Experimental Section and Figures S1−S15 in the Supporting Information for details).

X-ray-quality single crystals were obtained for compounds **1b**, **2a**, **3b**, and **4b** (Table 1, Figures 1−4). Slow diffusion of diisopropyl ether into an acetonitrile solution of **1b** and **3b**

Scheme 1. Synthesis of the Complexes 1b−5b

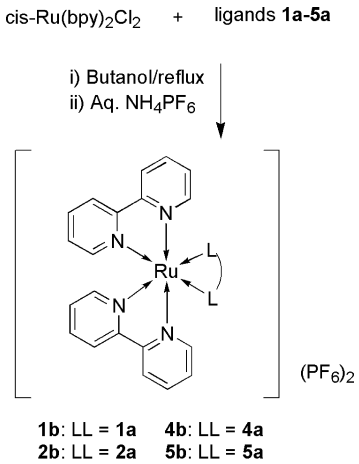

afforded the best single crystals, whereas crystals of **2a** and **4b** could be grown by sublimation of **2a** and slow diffusion of diethyl ether into an acetone solution of **4b**, respectively. Ligand **2a** and complexes **1b** and **3b** crystallize in the monoclinic crystal system, while complex **4b** crystallizes in the triclinic crystal system. The crystallographic data are summarized in Table 1 (see Figure S16 (Supporting Information) for the packing of ligand **2a** and Table S1 (Supporting Information) for selected bond angles and distances in comparison to the same by DFT calculations). In ligand **2a**, the guanidine moiety adopts a more stable twisted-chair conformation instead of the boat conformation (Figure 1). To minimize the lone pair-lone pair repulsion, atoms N1 and N4 adopt a trans geometry around the C8−N3 bond. The N3−C1 (1.413(4) Å) and N2−C1 (1.391(3) Å) bond distances clearly suggest that there is delocalization around the N3−C1−N2 core, whereas N1−C1 seems to be a localized C−N double bond with a distance of 1.283(4) Å. Extensive $\pi-\pi$ interactions between the aromatic rings, noncovalent solid-state Br−Br interactions, and aromatic C−H−Br interactions along with aromatic C−H−N interactions all play a role in the solid-state packing of molecule **2a** (see Figure S16 in the Supporting Information).

Complexes **1b**, **3b**, and **4b** exhibit coordinatively saturated ruthenium atoms in a distorted-octahedral geometry, with four nitrogen atoms of two bpy ligands, one nitrogen from guanidine, and another nitrogen from the pyridine, pyrimidine,[21] or chloropyrimidine moiety, respectively (Figures 2, 3 and 4 for X-ray structures of **1b**, **4b** and **3b**, respectively).

The distortion from a regular octahedron is due to the smaller ligand bite angles at the metal center formed by the two 2,2′-bipyridine ligands. Selected bond distances and angles are tabulated for compounds **1b**, **3b**,[21] and **4b** in observance with the values obtained from DFT calculation (see Table S1 in the Supporting Information). The average bite angles for the bpys are 80.45(3), 78.82(9), and 78.85(2)° for compounds **1b**, **3b**, and **4b**, respectively. In general, the average of the aforementioned bite angles N−Ru−N (average = 79.37°) is lower by 5° than the average value observed in other Ru complexes containing two bpys as ligands (average = 84.8(5)°).[24] In the complexes, the bicyclic ligands **1a**, **3a**, and **4a** adopt six-membered twisted-chair chelate ring conformations, having bite angles of 82.8(3), 84.9(8), and 85.2(1)°, respectively. This gradual increase in bite angle with decreasing

dx.doi.org/10.1021/ic4028332 | *Inorg. Chem.* 2014, 53, 1679−1689

Table 1. Crystal Data and Details of the Structure Determination for 2a, 1b, 3b, and 4b·5C_3H_6O·2H_2O

	2a	1b	3b	4b·5C_3H_6O·2H_2O
formula	$C_{12}H_{15}N_4Br$	$[C_{32}H_{32}N_8Ru][PF_6]_2$	$[C_{31}H_{31}N_9Ru][PF_6]_2$	$[C_{31}H_{30}N_9ClRu][PF_6]_2[5C_3H_6O][2H_2O]$
M_w; d_{calcd} (g/cm^3)	295.19; 1.648	919.67; 1.688	920.66; 1.739	1281.52; 2.011
T (K); F(000)	100; 600	150; 3696	150; 1848	150; 1020
cryst syst	monoclinic	monoclinic	monoclinic	triclinic
space group	$P2_1/n$	$C2/c$	$P2_1/c$	$P\bar{1}$
unit cell				
a (Å)	5.0181(2)	35.651(1)	20.4021(8)	12.0837(5)
b (Å)	18.1139(6)	10.1520(3)	10.5565(4)	12.3164(4)
c (Å)	13.0979(4)	26.151(1)	16.4117(7)	14.5069(5)
α (deg)	90	90	90	88.110(2)
β (deg)	92.255(2)	130.121(1)	95.787(2)	81.464(2)
γ (deg)	90	90	90	82.341(2)
V (Å^3); Z	1189.64(7)	7273.7(4); 8	3516.7(2); 4	2115.87(13); 2
θ range (deg); completeness	4.17−70.95; 0.977	3.4−72.31; 0.87	2.18−72.54; 0.977	3.08−69.33; 0.980
no. of collected/indep rflns; R_{int}	2237/1898; 0.0689	7142/5287; 0.10	6818/5887; 0.057	7827/7508; 0.045
μ (mm^{-1})	4.566	5.252	5.414	5.144
R1(F); wR2(F^2); GOF(F^2)[a]	0.0366; 0.0950; 1.028	0.0640; 0.1889; 0.98	0.0415; 0.0971; 1.038	0.0611; 0.1867; 1.089
residual electron density	0.936; −0.763	3.297; −1.092	0.882; −0.827	1.532; −1.016

[a]R1(F) based on observed reflections with $I > 2\sigma(I)$ for **1b** and **3b** and $I > 4\sigma(I)$ for **2a** and **4b**; wR2(F^2) and GOF(F^2) based on all data for all compounds.

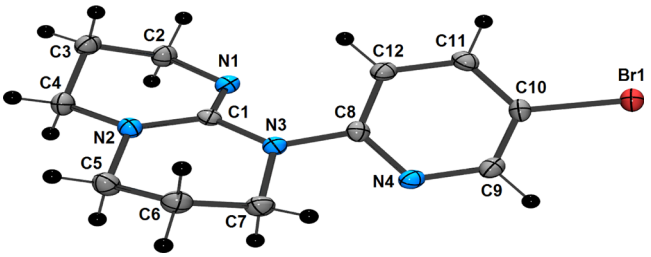

Figure 1. Crystal structure of ligand **2a**. Thermal ellipsoids are shown at the 50% probability level.

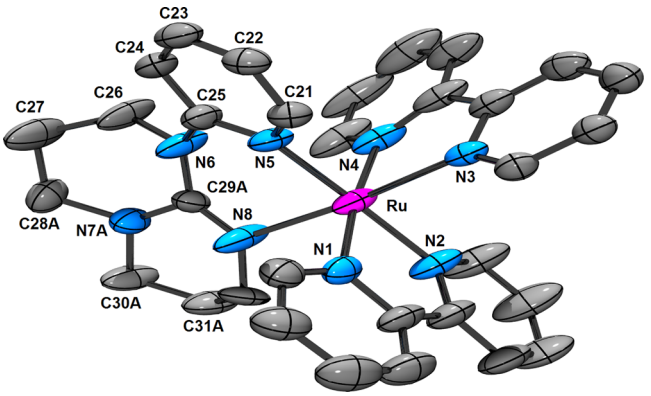

Figure 2. Crystal structure of **1b**. Hydrogen atoms, PF_6 anions, and a disordered part of the guanidine moiety are omitted for clarity. Thermal ellipsoids are shown at the 50% probability level.

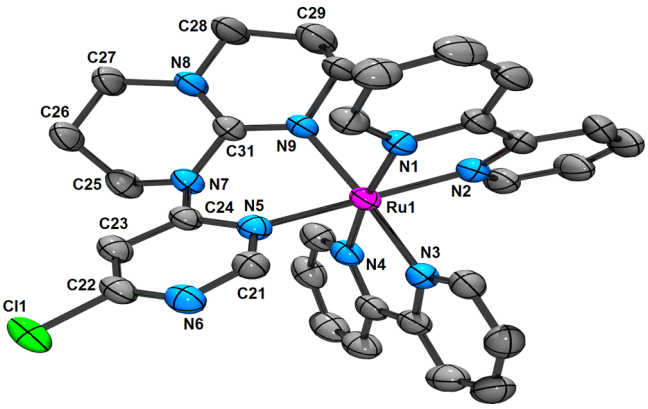

Figure 3. Crystal structure of **4b**. Hydrogen atoms, solvated acetone, and PF_6 anions are omitted for clarity. Thermal ellipsoids are shown at the 50% probability level.

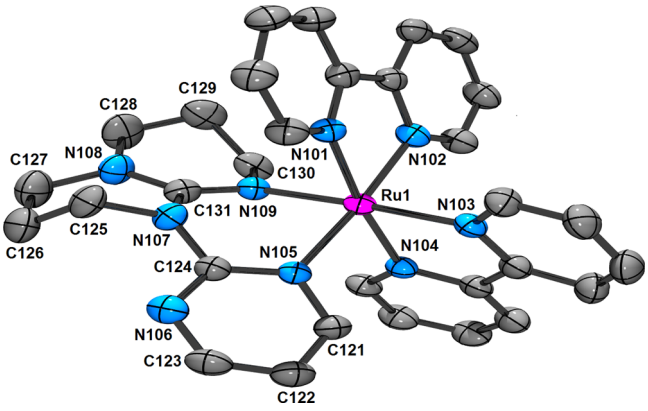

Figure 4. Crystal structure of **3b**. Hydrogen atoms and PF_6 anions are omitted for clarity. Thermal ellipsoids are shown at the 50% probability level. Structure is redrawn using crystal data in ref 21.

nucleophilicity of the ligands, from **1a** to **3a** to **4a**, suggests that the angle opens up due to less strong bonding of the heterocyclic ligands. The six Ru−N distances range between 1.992(6) and 2.187(7) Å, between 2.051(2) and 2.090(2) Å, and between 2.054(4) and 2.090(4) Å for compounds **1b**, **3b** and **4b**, respectively. The Ru−N distances for the coordinated bpy ligands are mainly the same for compound **1b** and are to some extent different for compounds **3b** and **4b**, whereas the averages for Ru−N were found to be almost the same for compounds **1b**, **3b**, and **4b** (2.056, 2.060, and 2.059 Å, respectively). These values are intermediate of the distances

dx.doi.org/10.1021/ic4028332 | Inorg. Chem. 2014, 53, 1679−1689

Table 2. Redox Data of Complexes 1b−5b in Dry, Degassed Acetonitrile[a]

	$E_{1/2}$(ox)	$E_{1/2}$(red)			$\Delta E_{1/2}$
1b	0.73 (100)	−1.41 (82)	−1.66 (86)	−2.30 (irr)[b]	2.14
2b	0.73 (105)	−1.40 (82)	−1.67 (210)		2.13
3b	0.75 (90)	−1.42 (62)	−1.63 (133)	−1.96 (145)	2.17
4b	0.78 (69)	−1.37 (71)	−1.63 (90)	−1.86 (irr)	2.15
5b	0.79 (92)	−1.24 (85)	−1.69 (130)	−1.97 (160)	2.03
$Ru(bpy)_3^{2+}$	1.27[c]	−1.35[c]	−1.55[c]	−1.76[c]	2.62
$Ru(bpy)_2(en)^{2+}$	0.96[d]	−1.46[d]	−1.71[d]		2.42
$Ru(bpy)_2(AEtPy)^{2+}$	1.12[e]	−1.41[e]	−1.63[e]		2.53

[a] $\Delta E_{1/2}$ is the difference (in mV) between the oxidation and first reduction potentials. Potentials are in volts vs SCE for acetonitrile solutions, 0.1 M in [*n*-Bu_4N]PF_6, recorded at 25 ± 1 °C at a sweep rate as mentioned in the text. The difference between the cathodic and anodic peak potentials (in millivolts) is given in parentheses. $\Delta E_{1/2}$ (in volts) for each compound is the difference between the first oxidation potential and the first reduction potential. [b] Irreversible; potential is given for the anodic wave. [c] From refs 26−28. [d] From ref 26 (en is ethylenediamine). [e] From ref 29 (AEtPy is aminoethylpyridine).

observed in Ru-bpy complexes in general (1.96−2.16 Å, average = 2.06(5) Å).[24]

In compound **3b**, the N107−C124 (1.392(3) Å) and N107−C131 (1.408(3) Å) bond distances clearly suggests that there is delocalization between the pyrimidine ring and guanidine to some extent, whereas N109−C131 appears to be a localized C−N double bond with a distance of 1.314(4) Å. Delocalization between the pyridine ring and guanidine moiety is also observed in compound **1b**, as revealed by N6−C25 (1.418(10) Å) and N6−C29* (1.40(3) Å) (the asterisk denotes the bond average of N6−C29A and N6−C29B; for clarity C29B is not shown in Figure 2) bond distances. Double-bond character is observed in the N8−C29** (1.32(2) Å) (the double asterisk denotes the bond average of N8−C29A and N8−C29B) bond in compound **1b**. The delocalization is limited for compound **4b**, as revealed by the C−N bond distances in **4b** (N7−C24 1.377(6) Å and N7−C31 1.421(6) Å). The bond distances suggest that N9−C31 (1.301(6) Å) has more localized C−N double-bond character in compound **4b**. The alkyl chains are directed away from the Ru(II) center, and thus the conformation of the saturated ring does not appear to have any noticeable influence on the structure, as opposed to other coordination complexes incorporating CH_2-bridged donor atoms.[25]

The redox behavior of complexes **1b**−**5b** has been examined by cyclic voltammetry using a glassy-carbon electrode in purified acetonitrile containing [*n*-Bu_4N]PF_6 as the supporting electrolyte versus Fc^+/Fc as the internal standard, under a dry argon atmosphere ,and data are gathered in Table 2. B3LYP density functional theory (DFT) calculations (see Figure 5 and the Supporting Information for computational details) predict that ligands **1a**−**5a** cause a significant destabilization of the HOMO, which is located principally on the ruthenium ion and partially on the ligand environment (see Figures S17−S19 in the Supporting Information). The oxidation process is therefore assigned to the removal of one electron from the metal-centered orbitals. The higher energies calculated for the HOMO of $[\mathbf{1b}]^{2+}$ (−5.51 eV), $[\mathbf{3b}]^{2+}$ (−5.64 eV), and $[\mathbf{4b}]^{2+}$ (−5.72 eV) in comparison with that of $[Ru(bpy)_3]^{2+}$ (−6.11 eV)[30] are in good agreement with the lower anodic potentials measured for **1b**, **3b**, and **4b** (Table 2) in comparison with $[Ru(bpy)_3]^{2+}$, as they clearly suggest strong σ donation from the saturated ligand backbone to the metal-based orbitals, thereby increasing the energy of the HOMO. This trend is in accord with the conclusions of Bolink et al.[31] At positive

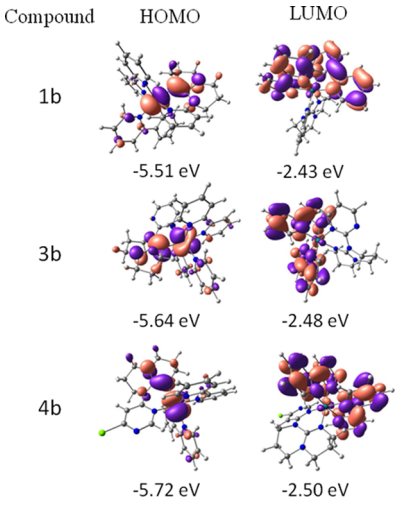

Figure 5. Kohn−Sham orbital sketches for HOMO and LUMO molecular orbitals for $\mathbf{1b}^{2+}$, $\mathbf{3b}^{2+}$, and $\mathbf{4b}^{2+}$ in the S = 0 ground state.

potentials, complexes **1b** (Figure 6) and **2b** show quasi-reversible Ru(II) to Ru(III) oxidations at 0.73 V vs SCE with a

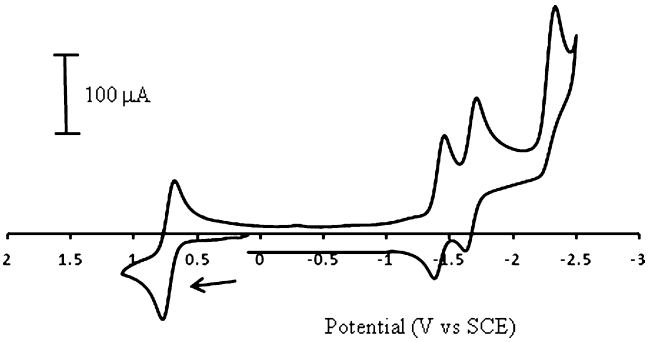

Figure 6. Cyclic voltammogram of **1b** (at 200 mV/s) in dry, degassed acetonitrile with 0.1 M $TBAPF_6$.

peak-to-peak separation (ΔE_p) of 100 mV at 200 mV/s. This value is 0.54 V less positive than that observed for the same Ru(III/II) couple in $[Ru(bpy)_3]^{2+}$, which appears at 1.27 V vs SCE:[26−28] i.e., **1b** is much easier to oxidize than $[Ru(bpy)_3]^{2+}$, confirming that **1a** is a stronger donor than bpy, although the effect of introducing an electron-withdrawing bromine atom does not seem to be so well pronounced for **2b**. Complex **3b**

dx.doi.org/10.1021/ic4028332 | Inorg. Chem. 2014, 53, 1679−1689

Table 3. Absorption Data in Deaerated CH_3CN Solutions for 1b−5b

	λ_{max}, nm ($10^{-3}\varepsilon$, M^{-1} cm^{-1})				
compound					
1b	242 (34.6)	293 (53.2)	357 (9.5)	487 (7.1)	560 (3.9)
2b	246 (23.3)	292 (31.8)	355 (4.8)	474 (4.4)	546 (2.3)
3b	241 (30.5)	293 (41.4)	350 (6.7)	474 (6.4)	550 (2.9)
4b	246 (16.4)	292 (26.6)	356 (4.1)	463 (4.1)	532 (2.1)
5b	244 (24.5)	291 (42.9)	357 (5.1)	468 (7.5)	531 (5.2)
$Ru(bpy)_3^{2+}$				450 (14)[a]	

[a]From ref 33a.

also shows a quasi-reversible Ru(III/II) couple at 0.75 V vs SCE (ΔE_p = 90 mV). This marginal increase in the Ru(III/II) couple in **3b** in comparison to that in **1b** may be attributed to the substitution of the pyridine donor in **1a** with a pyrimidine in **3a**. As pyrimidine is a weaker donor ligand, the Ru center in **3b** is more difficult to oxidize.[12,32] Complex **4b** presents a well-defined reversible peak at 0.78 V, with respect to the SCE, with a peak-to-peak separation of 69 mV. The oxidation peak of **4b** is more positively shifted by 50 and 30 mV in comparison to **1b** (also **2b**) and **3b**, respectively, indicating the electron-withdrawing nature of the chlorine atom. Complex **5b** exhibits a one-electron quasi-reversible Ru(III/II) couple at 0.79 V (ΔE_p = 92 mV) vs SCE. This value is 60, 40, and 10 mV more positive with respect to **1b** (also **2b**), **3b**, and **4b**, respectively. Since pyrazine is a weaker donor ligand in comparison to both pyrimidine and pyridine, the Ru(II) center in **5b** is more difficult to oxidize, and indeed it is the most difficult compound to oxidize in the series. It is worth noting that the new ligands **1a**−**5a** reported in this work are even more electron donating than 2-(2′-aminoethyl)pyridine (AEtPy) or ethylenediamine (en), as revealed by the Ru(III/II) couples of the complexes $Ru(bpy)_2(AEtPy)^{2+}$ (1.12 V vs SCE) and $Ru(bpy)_2(en)^{2+}$ (0.96 V vs SCE) reported in Table 2.

All of the complexes display ligand-based reduction peaks. The first two reduction peaks are assigned to bpy-based processes, by comparison of their potential values to those of $Ru(bpy)_3^{2+}$ (−1.35, −1.55, and −1.76 V vs SCE).[1b,27,28] DFT calculations confirm that the lowest unoccupied molecular orbital (LUMO) is fully localized on the bpy ligand for **1b** (−2.43 eV), **3b** (−2.48 eV), and **4b** (−2.50 eV) (Figures S17−S19 in the Supporting Information) and is calculated to be ∼0.04−0.11 eV higher than the LUMO of $[Ru(bpy)_3]^{2+}$ (−2.54 eV).[30] The destabilization of the LUMO explains the shifts of 60, 70, and 20 mV to more negative values measured for the first reduction potentials of **1b** (−1.41 V), **3b** (−1.42 V), and **4b** (−1.37 V) in comparison with that of $[Ru(bpy)_3]^{2+}$ (−1.35 V),[26] respectively. The sharp decrease of the first reduction potential of compound **5b** with respect to that of compound **4b** may be attributed to the poor nucleophilicity of **5a** in comparison to that of **4a**. As **5a** is less basic, the extent of back-bonding from the metal center to bpy will also be decreased; hence, the bpys are poor in electron density, thus rendering them easier to reduce. The third reduction peak for **1b** had an anodic peak potential of −2.30 V vs SCE, whereas that for **3b** is more well-defined and was centered at −1.96 V vs SCE. These peaks can be designated as reductions occurring at **1a** and **3a**, respectively. These peaks for **4b** and **5b** appear at −1.86 and −1.97 V vs SCE, respectively. As pyrimidine is a better π-acceptor than pyridine, it is easier to reduce ligand **3a** in complex **3b** than ligand **1a** in complex **1b**. Similarly, the chloro-substituted pyrimidine moiety in ligand **4a** is a better π acceptor than pyrimidine in **3a** and, thus, the third reduction for complex **4b** appears at more positive potential with respect to complex **3b**.

The electronic absorption spectra of ligands **1a**−**5a** are rather featureless and display conventional spin-allowed $\pi \rightarrow \pi^*$ transition(s) centered around 230−290 nm (see Table S2 in the Supporting Information).

The UV−vis absorption spectra of compounds **1b**−**5b** in acetonitrile solution (Table 3 and Figure 7) display spin-allowed ^{1}MLCT (metal to ligand charge transfer) bands in the 400−600 nm region. These bands correspond to electronic transitions from the HOMO to virtual unoccupied molecular orbitals. As suggested by TD-DFT calculations of $\mathbf{1b}^{2+}$, $\mathbf{3b}^{2+}$, and $\mathbf{4b}^{2+}$, the HOMOs of these compounds possess significant hpp character (27−29%) (Figures 8 and 9); however, assigning these transitions as metal−ligand to ligand charge transfer (^{1}(ML)-LCT) states instead of ^{1}MLCT states may not be appropriate either. The UV region is dominated by the $\pi \rightarrow \pi^*$ transition in the ligand (bpy) moieties centered around 290 nm for all of the compounds.[1b,7b,c] The most noticeable feature in the visible region of the electronic absorption spectra of the complexes is that the lowest-energy ^{1}MLCT maxima are red-shifted with respect to the ^{1}MLCT of $Ru(bpy)_3^{2+}$, and the amount of shift depends on the electronic properties of the heterocycle coupled with the guanidine moiety.[33] As ligands **1a**−**5a** are stronger donors than bpy, they are expected to interact with the d orbitals of ruthenium more strongly than bpy, raising the metal-based HOMO energy. This is perfectly in line with the DFT calculations reported above. On the other hand, the LUMO is still bpy-based, as also indicated by the first

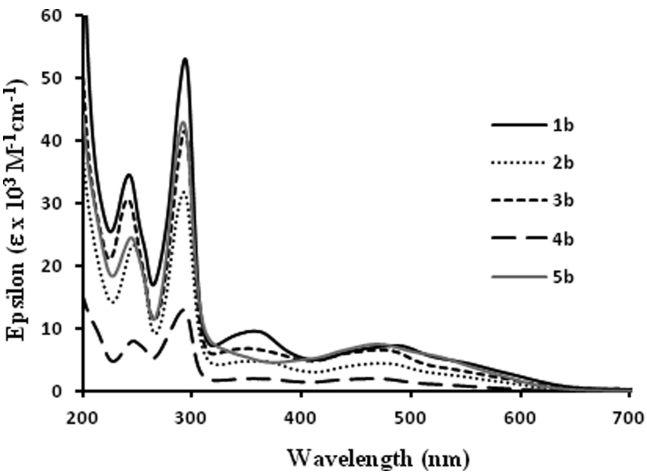

Figure 7. Electronic absorption spectra of compounds **1b**−**5b** at room temperature in deareated acetonitrile.

dx.doi.org/10.1021/ic4028332 | Inorg. Chem. 2014, 53, 1679−1689

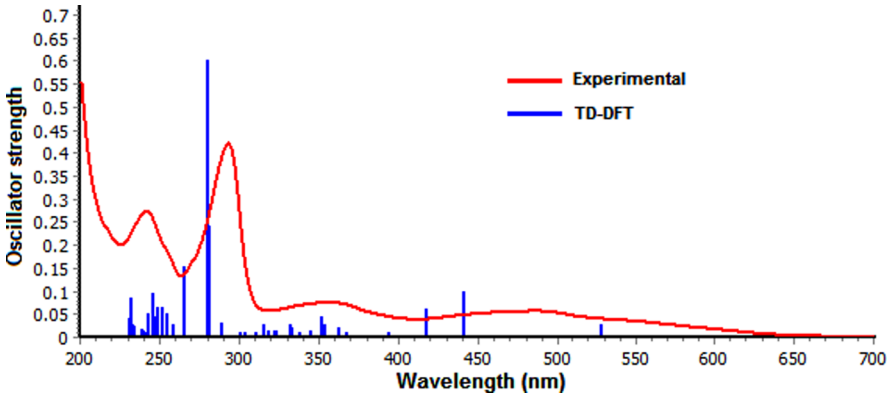

Figure 8. Typical figure showing the overlap of experimental electronic absorption spectra with oscillator strength from TD-DFT calculation of $\mathbf{1b}^{2+}$ in the $S = 0$ ground state.

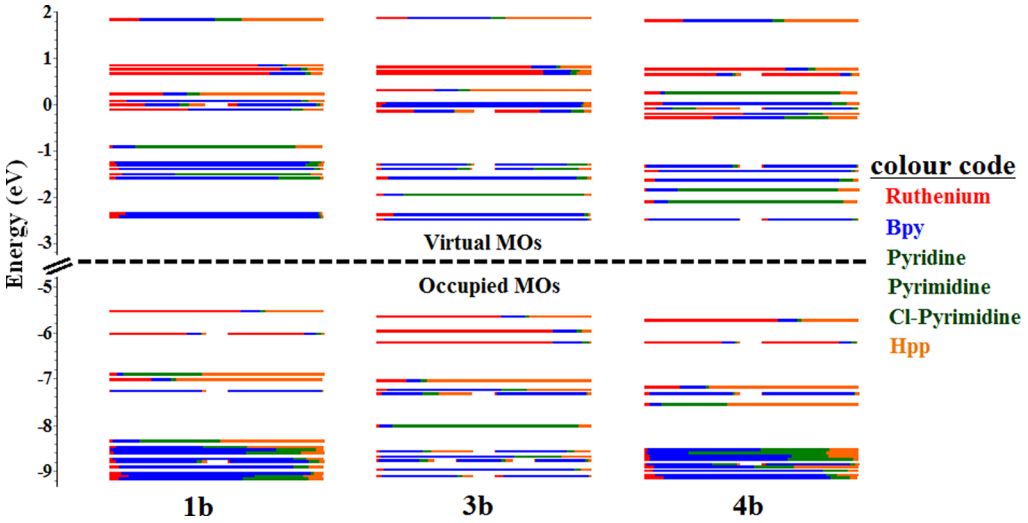

Figure 9. Calculated frontier MO energies of all the modeled complexes **1b**, **3b**, and **4b** obtained from DFT (rb3lyp/LanL2DZ(f) (Ru)/6-31G** (NCN) with CPCM (CH_3CN)) and a 0.05 eV threshold of degeneracy.

reduction potentials of **1b**−**5b**. This results in a lowering of the energy of the $d\pi \rightarrow \pi^*$ ^{1}MLCT transition and, hence, a red shift in the absorption spectra. As ligand **1a** is the strongest donor in the series **1a**−**5a**, complex **1b** displays a more pronounced red shift in its ^{1}MLCT in comparison to the other complexes (see the last column in Table 3). Ligand **2a** appears to have donor capacity equal to that of **3a** but more than that of ligands **4a** and **5a**, containing electron-withdrawing chloropyrimidine and pyrazine moieties, respectively. Moreover, the complexes show additional bands at approximately 350 nm, which receive contributions from a ^{1}MLCT transition involving the higher-energy orbital of bipyridine.[34] It may be noted that such a band is usually observed for $Ru(bpy)_2(diamine)^{2+}$ chromophores.[26]

The luminescence properties of all the complexes were studied in dry, degassed acetonitrile at room temperature. The corrected emission spectra maxima (λ_{max}) along with lifetime (τ), quantum yield (ϕ), and excited-state radiative (k_r) and nonradiative (k_{nr}) decay values are reported in Table 4, whereas the corrected spectra are shown in Figure 10. In all cases, the emission is attributed to a triplet Ru to bpy CT excited state. Interestingly, to the best of our knowledge, these are the lowest-energy Ru to bpy CT emissions for $Ru(bpy)_2(N\text{-}N)^{2+}$ compounds, where N-N is a neutral ligand, and demonstrate that anionic ligands are not strictly required to obtain a large

Table 4. Photophysical Data in Deaerated CH_3CN Solutions for Complexes 1b−5b

	luminescence[a] @ 298 K				
compound	λ_{max}, nm	τ, ns	$10^{-4}\phi$	$10^3 k_r$ (s^{-1})	$10^6 k_{nr}$ (s^{-1})
1b	745	54	3.4	6.3	18.5
2b	745	51	5.0	9.8	19.6
3b	740	73	3.6	4.9	13.7
4b	732	78	6.8	8.7	12.8
5b	736	67	5.5	8.2	14.9
$Ru(bpy)_3^{2+}$	620[b,c]	860[b]	620[b]	72.1	1.1

[a]Corrected for the photomultiplier response. [b]From ref 33a. [c]From ref 34.

red shift of ^{3}MLCT emissive states involving bpy. Concomitant with the bathochromic shift of the ^{1}MLCT absorption bands in the absorption spectra in comparison to that of $Ru(bpy)_3^{2+}$, there is a red shift in ^{3}MLCT emission bands in comparison to the emission of $Ru(bpy)_3^{2+}$. Of note, the emission maxima are red-shifted with an increase in basicity of the moiety containing the hpp subunit. The emission energy (λ_{max}, nm) and the energy gap as expressed by $\Delta E_{1/2}$ are correlated, albeit without solvation effects being taken into account. Indeed, the red shift of the Ru to bpy CT emission for all of the studied complexes in comparison to $[Ru(bpy)_3]^{2+}$ is due to the narrower

dx.doi.org/10.1021/ic4028332 | Inorg. Chem. 2014, 53, 1679−1689

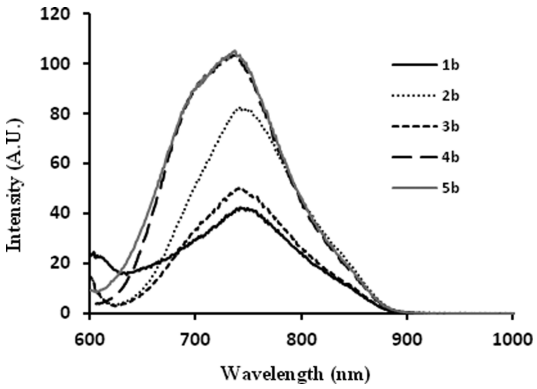

Figure 10. Emission spectra of compounds **1b**−**5b**, corrected for photomultiplier response.

HOMO−LUMO energy gaps calculated for $[\mathbf{1b}]^{2+}$ (3.08 eV), $[\mathbf{3b}]^{2+}$ (3.16 eV), and $[\mathbf{4b}]^{2+}$ (3.22 eV) in comparison to that of $[Ru(bpy)_3]^{2+}$ (3.57 eV),[31] thereby confirming the agreement among redox, TD-DFT, and emission data.

The red shift in emission energy is accompanied by a sharp decrease in emission quantum yield and lifetime in comparison to $Ru(bpy)_3^{2+}$ and similar species,[1b] as expected on the basis of the energy gap law.[7b,c,35,36] In heteroleptic Ru(II)−polypyridyl complexes, substituents with extended π systems permit greater delocalization of the excited MLCT state, with smaller bond displacement changes, and, a concomitant decrease in non-radiative decay, eventually allowing for relatively long lifetimes.[37,38] However, this is valid only when the acceptor ligand of the emissive ^{3}MLCT state is a large aromatic ligand, which is not occurring here, where the emitting ^{3}MLCT state is a bpy ligand in all of the complexes. Due to the presence of thermally accessible low-lying triplet metal-centered (^{3}MC) states close to the radiative ^{3}MLCT states, the energy gap law, predicting a roughly inversed linear dependence of ln k_{nr} on the emission energy, is sometimes not followed by the luminescence properties of Ru(II) complexes at room temperature.[1b,7] However, in the present series of compounds, the inversed linear relationship between ln k_{nr} and the emission energy (in cm^{-1}) is roughly kept—also considering the experimental uncertainties in lifetime and quantum yield determination—suggesting that the energy gap law plays a significant role in determining the excited-state lifetime.

Finally, a cursory look at the data in Table 4 also indicates that the radiative decay constants of **1b**−**5b** are 1 order of magnitude smaller than that of $Ru(bpy)_3^{2+}$. Of course, this negatively affects the luminescence performance of the compounds, in particular quantum yield data. Lower values are also found (see data in Table 3) for the molar absorption coefficient of the lowest-energy ^{1}MLCT bands of the new compounds (around 5000 M^{-1} cm^{-1}) in comparison to the MLCT of $Ru(bpy)_3^{2+}$ (about 15000 M^{-1} cm^{-1}). Although the emission process refers to a triplet ^{3}MLCT state and the absorption to the corresponding singlet state, the combination of molar absorption coefficient and radiative decay data suggests that the oscillator strength(s) of MLCT transitions in **1b**−**5b** are smaller than in $Ru(bpy)_3^{2+}$. A possible explanation lies in the distortion from the octahedral arrangement around the metal center, which is larger in **1b**−**5b** than in the prototype $Ru(bpy)_3^{2+}$ compound, as indicated by the crystal structure data of **2b**−**4b**, reported above. Such an increased octahedral distortion would negatively affect metal and bpy orbital overlaps, thus decreasing the oscillator strength and therefore the probability of ^{1}MLCT transitions.

CONCLUSION

In conclusion, five novel N_{amine}-substituted guanidine-pyridine/pyrimidine/pyrazine ligands were synthesized and their coordination to ruthenium(II) formed stable six-membered chelate rings. From the Ru(III/II) potentials of the new complexes, it is found that all the new ligands possess strong donating ability in comparison to common polypyridyls: e.g., bpy and phenanthroline. In fact, the ligands reported in this work are even more electron donating than 2-(2′-aminoethyl)-pyridine (AEtPy) or ethylenediamine (en), as revealed by the Ru(III/II) couples of the complexes $Ru(bpy)_2(AEtPy)^{2+}$ (1.12 V vs SCE) and $Ru(bpy)_2(en)^{2+}$ (0.96 V vs SCE).[26,29,39] As a result of strong σ donation from the ligands, complexes **1b**−**5b** have low-energy ^{1}MLCT absorptions in the visible region in comparison to $Ru(bpy)_3^{2+}$. The 298 K fluid solution emission maxima for the complexes are also red-shifted by ∼100 nm with respect to that for $Ru(bpy)_3^{2+}$, and they arise due to Ru^{II} to bpy ^{3}MLCT states, since the π^* orbitals are predominantly bpy based, as evidenced by DFT calculations. Thus, the complexes, having interesting photophysical and unique redox properties, can serve as excellent red-absorbing and light-harvesting materials.

EXPERIMENTAL SECTION

For materials, methods, and instrumentation see the Supporting Information.

Syntheses of the Compounds. *1-(Pyridin-2-yl)-2,3,4,6,7,8-hexahydro-1H-pyrimido[1,2-a]pyrimidine (**1a**).* (±)-BINAP (0.06 mmol, 38 mg) was placed in a oven-dried round bottomed flask, which was purged with argon and sealed with a septum. Dry toluene (3 mL) was injected inside. The resulting suspension was heated at 90 °C for 2 min to dissolve the BINAP. This mixture was cooled to room temperature, $Pd(OAc)_2$ (0.04 mmol, 9 mg) was added, and the mixture was stirred for 3 min. To the resulting bright yellow solution were added 2-bromopyridine (4 mmol, 0.38 mL) and 1,3,4,6,7,8-hexahydro-2*H*-pyrimido[1,2-*a*]pyrimidine (4.3 mmol, 600 mg). Stirring for 5 min at ambient temperature resulted in a pale orange slurry, to which was added *t*-BuOK (5.6 mmol, 640 mg). The flask was again purged with argon, and the reaction mixture was then stirred at 90 °C for 3 h, after which time it was cooled to room temperature and diethyl ether (60 mL) was added and the solution was filtered. Evaporation of the filtrate gave the ligand as a yellow oil. Yield: 780 mg (90%). ^{1}H NMR ($CDCl_3$, 300 MHz): 8.24 (dd, J^d = 6.0 Hz, J^d = 2.0 Hz, 1 H), 7.65 (d, J^d = 8.0 Hz, 1 H), 7.47 (td, J^t = 6.0 Hz, J^d = 2.0 Hz, 1 H), 6.77 (td, J^t = 6.0 Hz, J^d = 2.0 Hz, 1 H), 3.87 (t, J^t = 6.0 Hz, 2 H), 3.41 (t, J^t = 6.0 Hz, 2 H), 3.21 (m, 4 H), 2.02 (quint, J^{qt} = 6.0 Hz, 2 H), 1.88 (quint, J^{qt} = 6.0 Hz, 2 H) ppm. ^{13}C NMR ($CDCl_3$, 75 MHz): 156.6, 149.9, 147.1, 135.9, 118.7, 116.9, 48.8, 48.6, 43.8, 43.7, 23.7, 22.7 ppm. HRMS (ESI), *m*/*z*: 217.14452 $[M + H^+]^+$ ($C_{12}H_{17}N_4$ requires 217.14477).

*1-(5-Bromopyridin-2-yl)-2,3,4,6,7,8-hexahydro-1H-pyrimido[1,2-a]pyrimidine (**2a**).* A 30 mL pressure tube with a stirring bar was charged with 2,5-dibromopyridine (474 mg, 2 mmol) and 1,3,4,6,7,8-hexahydro-2*H*-pyrimido[1,2-*a*]pyrimidine (557 mg, 4 mmol). The tube was sealed and heated to 90 °C in an oil bath for 3 h, after which time it was cooled to room temperature. Toluene (5 mL) was added to the resulting yellow mixture, followed by the addition of diethyl ether (40 mL). After filtration and evaporation of the solvents, a light yellow crystalline solid was obtained, which was dried under vacuum overnight. The product was purified by sublimation as a white crystalline solid. Yield: 568 mg (96%). ^{1}H NMR (400 MHz, $CDCl_3$): 8.27 (dd, J^{dd} = 0.5, 2.5 Hz, 1 H), 7.67 (dd, J^{dd} = 0.5, 9.0 Hz, 1 H), 7.55 (dd, J^{dd} = 2.5, 9.0 Hz, 1 H), 3.89−3.83 (m, 2 H), 3.42 (t, J^t = 6.0 Hz, 2 H), 3.32−3.27 (m, 4 H), 2.04 (quint, J^{qt} = 6.0 Hz, 2 H), 1.90 (quint,

dx.doi.org/10.1021/ic4028332 | Inorg. Chem. 2014, 53, 1679−1689

J^{qt} = 6.0 Hz, 2 H) ppm. ^{13}C NMR (100 MHz, $CDCl_3$): 154.9, 149.3, 147.3, 137.9, 119.7, 111.4, 48.5, 48.3, 43.6, 43.3, 23.3, 22.4 ppm. HRMS (ESI), *m/z*: 295.05554 $[M + H^+]^+$ ($C_{12}H_{16}BrN_4$ requires 295.05529). Anal. Calcd for $C_{12}H_{15}N_4Br$: C, 48.83; N, 18.98; H, 5.12. Found: C, 48.83; N, 18.79; H, 5.14.

*1-(Pyrimidin-2-yl)-2,3,4,6,7,8-hexahydro-1H-pyrimido[1,2-a]-pyrimidine (**3a**).* 1,3,4,6,7,8-Hexahydro-2*H*-pyrimido[1,2-*a*]pyrimidine (150 mg, 1.1 mmol) and 2-bromopyrimidine (160 mg, 1 mmol) were taken in a pressure tube and slowly heated to 130 °C, wherein a brown sticky solid was obtained. Heating was maintained at 130 °C for 1 h, after which time the tube was cooled to room temperature and the solid was purified by column chromatography on Al_2O_3 with 10% MeOH in $CHCl_3$ as eluent. The product was obtained by evaporation of the solvent and overnight drying under vacuum. Yield: 60 mg (55%). ^{1}H NMR ($CDCl_3$, 400 MHz): 8.72 (d, Hz, J^d = 5.0 Hz, 2 H), 7.17 (t, J^t = 5.0 Hz, 1 H), 4.34 (t, J^t = 6.0 Hz, 2 H), 3.75 (m, 4 H), 3.69 (t, J^t = 6.0 Hz, 2 H), 2.27 (quint, J^{qt} = 6.0 Hz, 2 H), 2.18 (quint, J^{qt} = 6.0 Hz, 2 H) ppm. ^{13}C NMR ($CDCl_3$, 75 MHz): 158.3, 157.7, 151.2, 117.1, 48.7, 43.7, 39.1, 20.8, 19.5 ppm. HRMS (ESI), *m/z*: 218.13925 $[M + H^+]^+$ ($C_{11}H_{16}N_5$ requires 218.14002).

*1-(6-Chloropyrimidin-4-yl)-2,3,4,6,7,8-hexahydro-1H-pyrimido-[1,2-a]pyrimidine (**4a**).* A 25 mL microwave tube was charged with 4,6-dichloropyrimidine (152 mg, 1 mmol) and 1,3,4,6,7,8-hexahydro-2*H*-pyrimido[1,2-*a*]pyrimidine (282 mg, 2 mmol). To this mixture was added toluene (15 mL). The tube was placed in a 400 MW microwave reactor and heated to 160 °C for 2 h. After the completion of the reaction, the solvent was decanted out and evaporated to dryness under reduced pressure. The product was purified by overnight sublimation at 1.8 mbar and 100 °C followed by recrystallization by slow diffusion of hexane in chloroform. The product was obtained as a pale yellow microcrystalline solid. Yield: 652 mg (92%). ^{1}H NMR ($CDCl_3$, 400 MHz): 8.51 (d, J^d = 0.9 Hz, 1 H), 7.93 (d, J^d = 0.9 Hz, 1 H), 4.02 (t, J^t = 6.0 Hz, 2 H), 3.51 (t, J^t = 6.0 Hz, 2 H), 3.27 (t, J^t = 6.0 Hz, 2 H), 3.18 (t, J^t = 6.0 Hz, 2 H), 2.01 (quint, J^{qt} = 6.0 Hz, 2 H), 1.92 (quint, J^{qt} = 6.0 Hz, 2 H) ppm. ^{13}C NMR ($CDCl_3$, 100 MHz): 161.5, 159.3, 157.7, 147.9, 110.3, 48.64, 48.61, 43.8, 42.6, 23.6, 22.3 ppm. HRMS (ESI), *m/z*: 252.10105 $[M + H^+]^+$ ($C_{11}H_{15}N_5Cl^{35}$ requires 252.10158); 254.09860 $[M + H^+]^+$ ($C_{11}H_{15}N_5Cl^{37}$ requires 254.10158).

*1-(Pyrazin-2-yl)-2,3,4,6,7,8-hexahydro-1H-pyrimido[1,2-a]-pyrimidine (**5a**).* A 30 mL pressure tube with a stirring bar was charged with 1,3,4,6,7,8-hexahydro-2*H*-pyrimido[1,2-*a*]pyrimidine (292 mg, 2.1 mmol), and 2-chloropyrazine (115 mg, 1 mmol) was added dropwise. The tube was sealed and heated at 95 °C in an oil bath for 3 h, after which time it was cooled to room temperature. Toluene (6 mL) was added to the resulting yellow viscous oil, followed by diethyl ether (40 mL). After filtration and evaporation of the solvents, the product was obtained as a colorless oil, which could be solidified by keeping the oil at −20 °C for 1 week to give a pale yellow solid. The solid was dissolved in a minimal volume of dichloromethane and filtered through a plug of Celite to give a clear colorless solution. Upon evaporation of the solvent under reduced pressure, a colorless oil was obtained. The oil was solidified at −20 °C and then dried under vacuum to furnish the product as a colorless solid. Yield: 189 mg (87%). ^{1}H NMR (400 MHz, $CDCl_3$): 9.06 (d, J^d = 1.2 Hz, 1 H), 8.12 (dd, J^{dd} = 1.2, 4.0 Hz, 1 H), 7.94 (d, J^d = 2.4 Hz, 1 H), 3.83 (t, J^t = 6.0 Hz, 2 H), 3.42 (t, J^t = 6.0 Hz, 2 H), 3.25 (t, J^t = 6.0 Hz, 2 H), 3.21 (t, J^t = 6.0 Hz, 2 H), 2.05 (quint, J^{qt} = 6.0 Hz, 2 H), 1.90 (quint, J^{qt} = 6.0 Hz, 2 H) ppm. ^{13}C NMR (100 MHz, $CDCl_3$): 152.9, 148.7, 141.9, 140.6, 135.2, 48.6, 48.4, 43.6, 42.8, 23.4, 22.5 ppm. HRMS (ESI), *m/z*: 218.13975 $[M + H^+]^+$ ($C_{11}H_{16}N_5$ requires 218.14002).

*[Ru(bpy)$_2$(**1a**)](PF$_6$)$_2$ (**1b**).* A 100 mL round-bottomed flask was charged with **1a** (0.22 mmol, 50 mg), *cis*-$Ru(bpy)_2Cl_2\cdot 2H_2O$ (0.2 mmol, 104 mg), and 1-butanol (10 mL), and the resulting dark purple solution was heated to reflux for 30 min. After it was cooled to ambient temperature, the dark solution was added dropwise to 50 mL of diethyl ether with vigorous stirring. A dark purple gum formed. The supernatant liquid was decanted, and the gum was dissolved in 10 mL of methanol. To this solution was added dropwise an aqueous solution of NH_4PF_6 (200 mg in 5 mL of water) with constant stirring. A dark precipitate appeared immediately. This was allowed to stand for 1 h, filtered, and then washed with water (20 mL) and diethyl ether (20 mL) and air-dried. Crystals suitable for X-ray crystallography were grown by diffusion of isopropyl ether into a moderately concentrated solution of the complex in acetonitrile. Yield: 110 mg (60%). ^{1}H NMR ($CDCl_3$, 700 MHz): 8.74 (d, J^d = 5.0 Hz, 1 H), 8.53 (d, J^d = 8.0 Hz, 1 H), 8.50 (d, J^d = 8.0 Hz, 1 H), 8.42 (m, 2 H), 8.37 (d, J^d = 8.0 Hz, 1 H), 8.13 (m, 2 H), 7.88 (m, 2 H), 7.80 (td, J^t = 8.0 Hz, J^d = 2.0 Hz, 1 H), 7.65 (m, 2 H), 7.59 (m, 2 H), 7.35 (d, J^d = 8.0 Hz, 1 H), 7.22 (t, J^t = 7.0 Hz, 1 H), 7.19 (t, J^t = 7.0 Hz, 1 H), 7.09 (d, J^d = 5.0 Hz, 1 H) 6.80 (td, J^t = 7.0 Hz, J^d = 1.0 Hz, 1 H), 3.79 (m, 1 H), 3.36 (m, 1 H), 3.18 (m, 3 H), 3.04 (m, 1 H), 2.91 (m, 1 H), 2.34 (m, 1 H), 2.25 (m, 1 H), 2.12 (m, 1 H), 1.63 (m, 1 H), 1.08 (m, 1 H) ppm. ^{13}C NMR ($CDCl_3$, 175 MHz): 158.8, 158.6, 158.5, 158.4, 157.7, 153.85, 153.81, 153.4, 152.7, 152.6, 151.2, 139.9, 137.9, 137.6, 137.3, 137.1, 127.6, 127.5, 127.1, 125.2, 125.1, 124.6, 124.2, 121.8, 117.3, 49.2, 49.1, 48.5, 47.9, 23.5, 23.3 ppm. HRMS (ESI), *m/z*: 775.14399 $[M - PF_6]^+$ ($C_{32}H_{32}N_8PF_6Ru$ requires 775.14297), 315.09062 $[M - 2PF_6]^{2+}$ ($C_{32}H_{32}N_8Ru$ requires 315.08912). Anal. Calcd for $C_{32}H_{32}N_8RuP_2F_{12}$: C, 41.79; H, 3.51; N, 12.18. Found: C, 41.70; H, 3.31; N, 11.95.

*[Ru(bpy)$_2$(**2a**)](PF$_6$)$_2$ (**2b**).* Ligand **2a** (65 mg, 0.22 mmol) and *cis*-$Ru(bpy)_2Cl_2\cdot 2H_2O$ (104 mg, 0.2 mmol) were dissolved in 1-butanol (15 mL) in a 50 mL round-bottomed flask, and the resulting dark purple solution was heated to reflux. The reaction was followed by TLC. After 3 h, the brown-red solution was cooled to room temperature. The solvent was evaporated under reduced pressure, and the residue was dissolved in the minimum volume of methanol, and to this solution was added a saturated aqueous solution of ammonium hexafluorophosphate to give a brown-red precipitate, which was filtered. The product was purified by flash column chromatography on silica using 10% saturated aqueous KNO_3 in acetonitrile. The nitrate salt was metathesized to the PF_6 salt by addition of excess of solid KPF_6 to the aqueous solution of the product. The precipitate was then filtered and dried under vacuum to give the product. Yield: 141 mg (71%). ^{1}H NMR (400 MHz, CD_3CN): 8.79 (d, J^d = 5.8 Hz, 1 H), 8.54 (t, J^t = 8.9 Hz, 2 H), 8.42 (m, 3 H), 8.16 (m, 2 H), 7.92 (m, 3H), 7.71 (ddd, J^{ddd} = 1.4, 5.8, 7.5 Hz, 1 H), 7.64 (m, 3 H), 7.25 (m, 3 H), 7.12 (d, J^d = 2.0 Hz, 1 H), 3.75 (m, 1 H), 3.37 (m, 2 H), 3.21 (m, 3 H), 3.07 (td, J^{td} = 6.0, 12.0 Hz, 1 H), 2.84 (m, 1 H), 2.23 (m, 1 H), 2.12 (m, 1 H), 1.65 (m, 1 H), 1.14 (dd, J^{dd} = 3.5, 7.5 Hz, 1 H) ppm. ^{13}C NMR (100 MHz, CD_3CN): 158.6, 158.5, 158.4, 158.2, 157.2, 153.7, 153.6, 153.5, 152.8, 152.7, 150.9, 142.2, 138.3, 137.9, 137.5, 137.4, 127.7, 127.65, 127.63, 127.3, 125.2, 125.1, 124.7, 124.4, 124.2, 115.8, 49.2, 49.1, 48.5, 47.8, 23.3, 23.1 ppm. HRMS (ESI), *m/z*: 853.05265 $[M - PF_6]^+$ ($C_{32}H_{31}BrN_8PF_6Ru$ requires 853.05349), 354.04497 $[M - 2PF_6]^{2+}$ ($C_{32}H_{31}BrN_8Ru$ requires 354.04438). Anal. Calcd for $C_{32}H_{31}N_8BrRuP_2F_{12}$: C, 38.49; N, 11.22; H, 3.13. Found: C, 38.35; N, 11.25; H, 2.92.

*[Ru(bpy)$_2$(**3a**)](PF$_6$)$_2$ (**3b**).* A 100 mL round-bottomed flask was charged with **3a** (22 mg, 0.1 mmol) and *cis*-$Ru(bpy)_2Cl_2\cdot 2H_2O$ (50 mg, 0.1 mmol), and to it was added an aliquot of a 1/1 (v/v) 1-butanol/water mixture (10 mL). The resulting clear, dark purple solution was refluxed for 16 h. After it was cooled to ambient temperature, the solvent was evaporated. The residue was taken up in a 1/1 (v/v) methanol/water mixture and filtered. To the filtrate was added, dropwise, an aqueous solution of NH_4PF_6 (200 mg in 5 mL of water) with constant stirring, while no precipitate appeared immediately. The precipitate, which was observed after overnight standing, was filtered, washed with water (5 mL) and diethyl ether (20 mL), and air-dried. The crude product was dissolved in acetonitrile and purified by column chromotography (SiO_2; acetonitrile/saturated aqueous KNO_3 7/2 v/v). The third reddish purple band contained the product. The nitrate salt was metathesized to the PF_6 salt by addition of solid NH_4PF_6 to an aqueous solution of the product. The precipitate was then filtered and dried under vacuum to give the product. Yield: 21 mg (23%). ^{1}H NMR ($CDCl_3$, 700 MHz): 8.88 (d, J^d = 6.0 Hz, 1 H), 8.56 (dd, J^d = 5.0 Hz, J^d = 2.0 Hz, 1 H), 8.52 (m, 2 H), 8.46 (d, J^d = 8.0 Hz, 1 H), 8.39 (d, J^d = 8.0 Hz, 1 H), 8.35 (d, J^d =

dx.doi.org/10.1021/ic4028332 | Inorg. Chem. 2014, 53, 1679−1689

8.0 Hz, 1 H), 8.14 (m, 2 H), 7.88 (td, J^t = 8.0 Hz, J^d = 2.0 Hz, 1 H), 7.85 (td, J^t = 8.0 Hz, J^d = 2.0 Hz, 1 H), 7.67 (td, J^t = 8.0 Hz, J^d = 2.0 Hz, 1 H), 7.62 (m, 2 H), 7.58 (d, J^d = 6.0 Hz, 1 H), 7.50 (dd, J^d = 6.0 Hz, J^d = 2.0 Hz, 1 H), 7.20 (m, 2 H), 6.82 (dd, J^d = 6.0 Hz, J^d = 1.0 Hz, 1 H), 3.89 (m, 1 H), 3.52 (m, 1 H), 3.32 (m, 2 H), 3.22 (m, 2 H), 3.09 (m, 1 H), 2.72 (m, 1 H), 2.29 (m, 1 H), 2.17 (m, 1 H), 1.68 (m, 1 H), 1.25 (m, 1 H) ppm. ^{13}C NMR ($CDCl_3$, 175 MHz): 161.2, 160.8, 158.8, 158.6, 158.44, 158.41, 158.3, 153.9, 153.5, 152.6, 152.5, 152.4, 138.1, 137.9 137.4, 137.2, 127.7, 127.4, 127.2, 124.9, 124.8, 124.7, 124.4, 118.1, 49.5, 49.2, 47.9, 46.1, 23.1, 22.6. HRMS (ESI), *m/z*: 776.1382 $[M - PF_6]^+$ ($C_{31}H_{31}N_9PF_6Ru$ requires 776.13822), 315.58803 $[M - 2PF_6]^{2+}$ ($C_{31}H_{31}N_9Ru$ requires 315.58675).

*[Ru(bpy)$_2$(**4a**)](PF$_6$)$_2$ (**4b**).* Ligand **4a** (72 mg, 0.3 mmol) and *cis*-$Ru(bpy)_2Cl_2{\cdot}2H_2O$ (160 mg, 0.3 mmol) were taken up in a 1/1 (v/v) 1-butanol/water mixture (15 mL) in a round-bottomed flask, and the solution was refluxed for 8 h. After the mixture was cooled to ambient temperature, the solvent was evaporated to dryness under reduced pressure. The residue was dissolved in a minimum volume of methanol, and then to this solution was added a saturated aqueous solution of NH_4PF_6 (200 mg in 5 mL of water) to give a precipitate, which was filtered off. The product was purified by column chromotography (silica; saturated aqueous KNO_3/acetonitrile 1/3 v/v). The reddish brown band contained the desired product. The nitrate salt was metathesized to the PF_6 salt by addition of solid NH_4PF_6 to an aqueous solution of the product. The precipitate was then filtered and dried under vacuum to give the product. Crystals suitable for X-ray crystallography were grown by diffusion of diethyl ether into a moderately concentrated solution of the complex in acetone. Yield: 179 mg (62%). ^{1}H NMR (400 MHz, CD_3CN): 8.79 (d, J^d = 5.6 Hz, 1 H), 8.50 (m, 3 H), 8.38 (dd, J^{dd} = 8.0, 3.6 Hz, 2 H), 8.16 (t, J^t = 8.0 Hz, 2 H), 7.88 (m, 2 H), 7.60 (m, 5 H), 7.32 (s, 1 H), 7.13−7.27 (m, 2 H), 3.75 (dt, J^{dt} = 14.0, 4.0 Hz, 1 H), 3.33 (m, 6 H), 3.08 (m, 1 H), 2.77 (d, J^d = 4.0 Hz, 1 H), 2.28 (m, 1 H), 1.67 (m, 1 H), 1.25 (m, 1 H) ppm. ^{13}C NMR (100 MHz, CD_3CN): 171.8, 162.9, 160.1, 158.9, 158.8, 158.7, 158.6, 158.5, 153.9, 153.8, 152.9, 152.8, 152.7, 138.2, 137.9, 137.4, 137.3, 127.8, 127.7, 127.6, 127.4, 125.3, 124.9, 124.6, 97.1, 68.7, 48.3, 47.9, 31.4, 23.2, 23.0 ppm. HRMS (ESI), *m/z*: 810.10117 $[M - PF_6]^+$ ($C_{31}H_{30}N_9ClPF_6Ru$ requires 810.09925), 332.56806 $[M - 2PF_6]^{2+}$ ($C_{31}H_{30}ClN_9Ru$ requires 332.56726). Anal. Calcd for $C_{31}H_{30}N_9F_{12}P_2ClRu$: C, 38.98; N, 13.20; H, 3.17. Found: C, 38.90; N, 13.06; H, 3.22.

*[Ru(bpy)$_2$(**5a**)](PF$_6$)$_2$ (**5b**).* Ligand **5a** (48 mg, 0.22 mmol) and *cis*-$Ru(bpy)_2Cl_2{\cdot}2H_2O$ (104 mg, 0.2 mmol) were taken up in 1-butanol (15 mL) in a round-bottomed flask, and the solution was refluxed for 4 h. After evaporation of the solvent, the residue was dissolved in a minimum volume of methanol, and then to this solution was added a saturated aqueous solution of NH_4PF_6 (200 mg in 5 mL of water) to give a precipitate, which was filtered. The product was purified by column chromotography (silica; saturated aqueous KNO_3/acetonitrile 1/3 v/v). The brownish red band contained the desired product. The nitrate salt was metathesized to the PF_6 salt by addition of solid NH_4PF_6 to an aqueous solution of the product. The precipitate was then filtered and dried under vacuum to give the product. Yield: 138 mg (76%). ^{1}H NMR (400 MHz, CD_3CN): 8.72 (d, J^d = 5.0 Hz, 1 H), 8.58 (m, 2 H), 8.51 (m, 3 H), 8.41 (d, J^d = 8.0 Hz, 1 H), 8.18 (m, 2 H), 7.91 (m, 2 H), 7.86 (d, J^d = 3.5 Hz, 1 H), 7.70 (ddd, J^{ddd} = 1.3, 5.8, 7.4 Hz, 1 H), 7.61 (m, 3 H), 7.27 (ddd, J^{ddd} = 1.4, 5.8, 7.4 Hz, 1 H), 7.23 (ddd, J^{ddd} = 1.3, 5.8, 7.4 Hz, 1 H), 7.09 (d, J^d = 2.6 Hz, 1 H), 3.94 (m, 1 H), 3.37 (m, 2 H), 3.21 (m, 2 H), 3.07 (td, J^{td} = 6.0, 12.0 Hz, 1 H), 2.92 (m, 1 H), 2.16 (m, 1 H), 1.65 (ddd, J^{ddd} = 3.4, 6.7, 9.9 Hz, 1 H), 1.11 (m, 2 H), 0.87 (m, 1 H) ppm. ^{13}C NMR (100 MHz, CD_3CN): 158.6, 158.33, 158.30, 158.2, 154.4, 153.7, 153.4, 153.3, 152.7, 152.6, 144.7, 140.5, 139.4, 138.5, 138.1, 137.9, 137.5, 127.9, 127.7, 127.2, 125.4, 125.3, 124.8, 124.3, 106.9, 49.3, 49.2, 48.3, 48.1, 23.4, 23.3 ppm. HRMS (ESI), *m/z*: 776.13732 $[M - PF_6]^+$ ($C_{31}H_{31}N_9PF_6Ru$ requires 776.13822), 315.58713 $[M - 2PF_6]^{2+}$ ($C_{31}H_{31}N_9Ru$ requires 315.58675). Anal. Calcd for $C_{31}H_{31}F_{12}N_9P_2Ru$: : C, 40.44; N, 13.69; H, 3.39. Found: C, 40.57; N, 13.31; H, 3.50.

Computational Details. All calculations were performed with Gaussian03[40] employing the DFT method, the Becke three-parameter hybrid functional,[41] and Lee−Yang−Parr's gradient-corrected correlation functional (B3LYP).[42] Singlet ground state geometry optimizations for **1b**$^{2+}$, **3b**$^{2+}$, and **4b**$^{2+}$ were carried out at the (R)B3LYP level in the gas phase, using their respective crystallographic structures as starting points. All elements except Ru were assigned the 6-31G(d,f) basis set.[43] The double-ζ quality LANL2DZ ECP basis set[44] with an effective core potential and one additional f-type polarization was employed for the Ru atom. Vertical electronic excitations based on (R)B3LYP-optimized geometries were computed for **1b**$^{2+}$, **3b**$^{2+}$, and **4b**$^{2+}$ using the TD-DFT formalism[45a,b] in acetonitrile using the conductor-like polarizable continuum model (CPCM).[46a−c] The CPCM model for geometry optimization was not used as for closed-shell geometry optimization calculations; the effect of solvent has very little influence on the computed geometries, and this fact has well been established in a recent literature report.[47] In addition, to prove this fact, additional DFT and TD-DFT calculations were performed with one of the complexes (**1b**$^{2+}$) in the following way. (i) A DFT geometry optimization calculation was carried out, taking into account the possible effect of solvent (through a polarized continuum model using acetonitrile as solvent) and the bond distances and angles of this model were compared (Table S9, Supporting Information) to that of the DFT geometry optimized model, which does not incorporate the effect of solvent (i.e., without CPCM). The result shows little variation with respective to bond distances and angles, which is not a critical aspect in this work. (ii) A TD-DFT calculation of **1b**$^{2+}$ was carried out including CPCM (acetonitrile) starting with a geometry optimized model, which was performed including CPCM (acetonitrile), and the principal transitions with their respective oscillator strengths and major transitions with relative contributions are tabulated in Table S11 (Supporting Information). (iii) A TD-DFT calculation of **1b**$^{2+}$ excluding CPCM (i.e., under vacuum) was carried out starting with a geometry optimized model, which was performed excluding CPCM, and the principal transitions with respective oscillator strengths and major transitions with relative contributions are given in Table S12 (Supporting Information). A direct comparison among the wavelengths of principal transitions with oscillator strengths and nature of the transitions in Tables S10−S12 clearly indicate that, for the closed-shell geometry optimization, the effect of solvent (through a polarized continuum model) has little influence on computed geometries, as the wavelengths of a particular transition, calculated by these three different types of TD-DFT calculations, fall in the experimental error range (±2 nm as tabulated in the DFT section in the Supporting Information) except for the transition at 279 nm, for which the maximum variation is ±4 nm. Although the relative contributions and oscillator strengths vary little, the nature of the particular transition remains unchanged. Vibrational frequency calculations were performed to ensure that the optimized geometries represent the local minima and there are only positive eigenvalues. The electronic distribution and localization of the singlet excited states were visualized using the electron density difference maps (ED-DMs).[48] Gausssum 2.2 was employed to visualize the absorption spectra (simulated with Gaussian distribution with a full width at half-maximum (fwhm) set to 3000 cm^{-1}) and to calculate the fractional contributions of various groups to each molecular orbital. All calculated structures were visualized with ChemCraft.[49]

■ ASSOCIATED CONTENT

Ⓢ Supporting Information

CIF files, text, tables, and figures giving crystallographic data for CCDC files 954083−954086 and further details as noted in the text along with the computational data. This material is available free of charge via the Internet at http://pubs.acs.org.

■ AUTHOR INFORMATION

Corresponding Author

*E-mail for G.S.H.: garry.hanan@umontreal.ca.

Notes

The authors declare no competing financial interest.

■ ACKNOWLEDGMENTS

A.K.P. and G.S.H. thank the Natural Sciences and Engineering Research Council of Canada (NSERC) and Centre for Self-Assembled Chemical Structure (CSACS) for financial support. S.C. thanks the MIUR (PRIN 2010-11 and FIRB Nanosolar projects) for financial support. We also thank Johnson Matthey PLC for a generous loan of ruthenium trichloride.

■ REFERENCES

(1) (a) Balzani, V.; Scandola, F. *Supramolecular Photochemistry*; Horwood: Chichester, U.K., 1991. (b) Juris, A.; Balzani, V.; Barigelletti, F.; Campagna, S.; Belser, P.; von Zelewsky, A. *Coord. Chem. Rev.* **1988**, *84*, 85. (c) Balzani, V.; Juris, A.; Venturi, M.; Campagna, S.; Serroni, S. *Chem. Rev.* **1996**, *96*, 759. (d) Medlycott, E. A.; Hanan, G. S. *Chem. Soc. Rev.* **2005**, *34*, 133. (e) Medlycott, E. A.; Hanan, G. S. *Coord. Chem. Rev.* **2006**, *250*, 1763.

(2) (a) Concepcion, J. J.; Jurss, J. W.; Templeton, J. L.; Meyer, T. J. *J. Am. Chem. Soc.* **2008**, *130*, 16462. (b) Zong, R.; Thummel, R. P. *J. Am. Chem. Soc.* **2005**, *127*, 12802.

(3) (a) Balzani, V.; Barigelletti, F.; De Cola, L. *Top. Curr. Chem.* **1990**, *158*, 31. (b) Alstrum-Acevedo, J. H.; Brennaman, M. K.; Meyer, T. J. *Inorg. Chem.* **2005**, *44*, 6802.

(4) Nazeeruddin, M. K.; Kay, A.; Rodicio, I.; Humphrybaker, R.; Muller, E.; Liska, P.; Vlachopoulos, N.; Gratzel, M. *J. Am. Chem. Soc.* **1993**, *115*, 6382.

(5) Yam, V. W.-W.; Lo, K. K.-W. *Coord. Chem. Rev.* **1998**, *184*, 157 and references cited therein.

(6) MacDermott, G.; Prince, S. M.; Freer, A. A.; Hawthornthwaite-Lawless, A. M.; Papiz, M. Z.; Cogdell, R. J.; Isaacs, N. W. *Nature* **1995**, *374*, 517.

(7) (a) Kalyanasundaram, K.; Grätzel, M.; Nazeeruddin, M. K. *J. Chem. Soc., Dalton Trans.* **1991**, *23*, 343. (b) Sauvage, J. P.; Collin, J. P.; Chambron, J. C.; Guillerez, S.; Coudret, C.; Balzani, V.; Barigelletti, F.; DeCola, L.; Flamigni, L. *Chem. Rev.* **1994**, *94*, 993. (c) Meyer, T. J. *Pure Appl. Chem.* **1986**, *58*, 1193.

(8) Balzani, V.; Juris, A. *Coord. Chem. Rev.* **2001**, *211*, 97.

(9) Anderson, P. A.; Keene, F. R.; Meyer, T. J.; Moss, J. A.; Strouse, G. F.; Treadway, J. A. *Dalton Trans.* **2002**, *20*, 3820 and references cited therein.

(10) Kitamura, N.; Kawanishi, Y.; Tazuke, S. *Chem. Phys. Lett.* **1983**, *97*, 103.

(11) Rillema, D. P.; Allen, G.; Meyer, T. J.; Conrad, D. *Inorg. Chem.* **1983**, *22*, 1617.

(12) Ernst, S.; Kaim, W. *Inorg. Chem.* **1989**, *28*, 1520.

(13) Ioachim, E.; Medlycott, E. A.; Hanan, G. S.; Loiseau, F.; Campagna, S. *Inorg. Chim. Acta* **2006**, *359*, 766.

(14) Ioachim, E.; Medlycott, E. A.; Hanan, G. S.; Loiseau, F.; Ricevuto, V.; Campagna, S. *Inorg. Chem. Commun.* **2005**, *8*, 559.

(15) Cook, M. J.; Lewis, A. P.; McAuliffe, G. S. G.; Skarda, V.; Thompson, A. J.; Glasper, J. L.; Robbins, D. J. *J. Chem. Soc., Perkin Trans. 2* **1984**, , 1303.

(16) de Carvalho, I. M. M.; de Sousa Moreira, I.; Gehlen, M. H. *Inorg. Chem.* **2003**, *42*, 1525.

(17) Bergman, S. D.; Goldberg, I.; Barbieri, A.; Barigelletti, F.; Kol, M. *Inorg. Chem.* **2004**, *43*, 2355.

(18) Bergman, S. D.; Goldberg, I.; Barbieri, A.; Kol, M. *Inorg. Chem.* **2005**, *44*, 2513.

(19) Ruminski, R. R.; Deere, P. T.; Olive, M.; Serveiss, D. *Inorg. Chim. Acta* **1998**, *281*, 1.

(20) (a) Johansson, K. O.; Lotoski, J. A.; Tong, C. C.; Hanan, G. S. *Chem. Commun.* **2000**, *10*, 819. (b) Denti, G.; Campagna, S.; Sabatino, L.; Serroni, S.; Ciano, M.; Balzani, V. *Inorg. Chem.* **1990**, *29*, 4750.

(21) Nag, S.; Ferreira, J. G.; Chenneberg, L.; Ducharme, P. D.; Hanan, G. S.; Ganga, G. L.; Serroni, S.; Campagna, S. *Inorg. Chem.* **2011**, *50*, 7.

(22) Wolfe, J. P.; Buchwald, S. L. *J. Org. Chem.* **2000**, *65*, 1144.

(23) Oakley, S. H.; Coles, M. P.; Hitchcock, P. B. *Inorg. Chem.* **2004**, *43*, 7564.

(24) Based on 278 ruthenium complexes containing at least two bpy and two more substituents with N atoms coordinated to the metal in the Cambridge Structural Database: Allen, F. H. *Acta Crystallogr., Sect. B: Struct. Sci.* **2002**, *B58*, 380.

(25) (a) De Groot, B.; Hanan, G. S.; Loeb, S. J. *Inorg. Chem.* **1991**, *30*, 4644. (b) Giesbrecht, G. R.; Hanan, G. S.; Kickham, J. E.; Loeb, S. J. *Inorg. Chem.* **1992**, *31*, 3286.

(26) Aydin, N.; Schlaepfer, C. W. *Polyhedron* **2001**, *20*, 37.

(27) Ji, Z.; Huang, S. D.; Guadalupe, A. R. *Inorg. Chim. Acta* **2000**, *305*, 127.

(28) Tokel-Takvoryan, N. E.; Hemingway, R. E.; Bard, A. J. *J. Am. Chem. Soc.* **1973**, *95*, 6582.

(29) Konno, H.; Ishii, Y.; Sakamoto, K.; Ishitani, O. *Polyhedron* **2002**, *21*, 61.

(30) Gorelsky, S. I.; Lever, A. B. P. *J. Organomet. Chem.* **2001**, *635*, 187.

(31) Bolink, H. J.; Coronado, E.; D. Costa, R.; Gaviña, P.; Ortí, E.; Tatay, S. *Inorg. Chem.* **2009**, *48*, 3907.

(32) Donato, L.; McCusker, C. E.; Castellano, F. N.; Zysman-Colman, E. *Inorg. Chem.* **2013**, *52*, 8495.

(33) (a) Calvert, J. M.; Caspar, J. V.; Binstead, R. A.; Westmoreland, T. D.; Meyer, T. J. *J. Am. Chem. Soc.* **1982**, *104*, 6620. (b) Gorelsky, S. I.; Dodsworth, E. S.; Lever, A. B. P.; Vlcek, A. A. *Coord. Chem. Rev.* **1998**, *174*, 469. (c) Gorelsky, S. I.; Lever, A. B. P. *Coord. Chem. Rev.* **2000**, *208*, 153.

(34) Casper, J. V.; Meyer, T. J. *Inorg. Chem.* **1983**, *22*, 2444.

(35) Casper, J. V.; Kober, E. M.; Sullivan, B. P.; Meyer, T. J. *J. Am. Chem. Soc.* **1982**, *104*, 630.

(36) Claude, J. P.; Meyer, T. J. *J. Phys. Chem.* **1995**, *99*, 51.

(37) Fang, Y.-Q.; Taylor, N. J.; Hanan, G. S.; Loiseau, F.; Passalacqua, R.; Campagna, S.; Nierengarten, A.; Dorsselaer, A. V. *J. Am. Chem. Soc.* **2002**, *124*, 7912.

(38) Polson, M. I. J.; Medlycott, E. A.; Hanan, G. S.; Mikelsons, L.; Taylor, N. J.; Watanabe, M.; Tanaka, Y.; Loiseau, F.; Passalacqua, R.; Campagna, S. *Chem. Eur. J.* **2004**, *10*, 3640.

(39) Brown, G. M.; Weaver, T. R.; Keene, F. R.; Meyer, T. J. *Inorg. Chem.* **1976**, *15*, 190.

(40) Frisch, M. J.; Trucks, G. W.; Schlegel, H. B.; Scuseria, G. E.; Robb, M. A.; Cheeseman, J. R.; Montgomery, J. A.; Vreven, T. J.; Kudin, K. N.; Burant, J. C.; Millam, J. M.; S;, I. S; Tomasi, J.; Barone, V.; Mennucci, B.; Cossi, M.; Scalmani, G.; Rega, N.; Petersson, G. A.; Nakatsuji, H.; Hada, M.; Ehara, M.; Toyota, K.; Fukuda, R.; Hasegawa, J.; Ishida, M.; Nakajima, T.; Honda, Y.; Kitao, O.; Nakai, H.; Klene, M.; Li, X.; Knox, J. E.; Hratchian, H. P.; Cross, J. B.; Adamo, C.; Jaramillo, J.; Gomperts, R.; Startmann, R. E.; Yazyev, O.; Austin, A. J.; Cammi, R.; Pomelli, C.; Ochterski, J. W.; Ayala, P. Y.; Morokuma, K.; Voth, G. A.; Salvador, P.; Dannenberg, J. J.; Zakrzewski, V. G.; Dapprich, J. M.; Daniels, A. D.; Strain, M. C.; Farkas, O.; Malick, D. K.; Rabuck, A. D.; Raghavachari, K.; Foresman, J. B.; Ortiz, J. V.; Cui, Q.; Baboul, A. G.; Cliffors, S.; Cioslowski, J.; B;, S. B; Liu, G.; Liashenko, A.; Piskorz, I.; Komaromi, I.; L;, M. R; Fox, D. J.; Keith, T.; Al-Laham, M. A.; Peng, C. Y.; Manayakkara, A.; Challacombe, M.; Gill, P. M. W.; Johnson, B. G.; Chen, W.; Wong, M. W.; Gonzalez, C.; Pople, J. A. *Gaussian 2003, Revision C.02*; Gaussian Inc., Pittsburgh, PA, 2003.

(41) Becke, A. D. *J. Chem. Phys.* **1993**, *98*, 5648.

(42) Lee, C.; Yang, W.; Parr, R. G. *Phys. Rev. B: Condens. Matter* **1988**, *37*, 785.

(43) McLean, A. D.; Chandler, G. S. *J. Chem. Phys.* **1980**, *72*, 5639.

(44) Hay, P. J.; Wadt, W. R. *J. Chem. Phys.* **1985**, *82*, 270.

(45) (a) Casida, M. E.; Jamorski, C.; Casida, K. C.; Salahub, D. R. *J. Chem. Phys.* **1998**, *108*, 4439. (b) Stratmann, R. E.; Scuseria, G. E.; Frisch, M. J. *J. Chem. Phys.* **1998**, *109*, 8218.

(46) (a) Cossi, M.; Rega, N.; Scalmani, G.; Barone, V. *J. Comput. Chem.* **2003**, *24*, 669. (b) Cossi, M.; Barone, V. *J. Chem. Phys.* **2001**, *115*, 4708. (c) Barone, V.; Cossi, M. *J. Phys. Chem. A* **1998**, *102*, 1995.

(47) Dixon, I. M.; Alary, F.; Heully, J.-L. *Dalton Trans.* **2010**, *39*, 10959.

(48) Browne, W. R.; O'Boyle, N. M.; McGarvey, J. J.; Vos, J. G. *Chem. Soc. Rev.* **2005**, *34*, 641.
(49) Zhurko, D. A.; Zhurko, G. A. *ChemCraft 1.5*; Plimus: San Diego, CA; available at http://www.chemcraftprog.com.